HHS Public Access

Author manuscript

Nat Cell Biol. Author manuscript; available in PMC 2011 January 01.

Published in final edited form as:

Nat Cell Biol. 2010 July ; 12(7): 676–685. doi:10.1038/ncb2070.

The Matricellular Protein CCN1/CYR61 Induces Fibroblast Senescence and Restricts Fibrosis in Cutaneous Wound Healing

Joon-Il Jun[1] and **Lester F. Lau**[1,*]

[1]Department of Biochemistry and Molecular Genetics, University of Illinois at Chicago, 900 S. Ashland Avenue, Chicago, Illinois 60607-7170, USA

Abstract

Cellular senescence is a recognised mechanism of tumor suppression; however, its contribution to other pathologies is not well understood. We show that the matricellular protein CCN1/CYR61, which is dynamically expressed at sites of wound repair, can induce fibroblast senescence through its cell adhesion receptors, integrin $\alpha_6\beta_1$ and heparan sulfate proteoglycans. CCN1 induces DNA damage response and p53 activation, and activates the RAC1-NOX1 complex to induce reactive oxygen species (ROS) generation and ROS-dependent activation of the $p16^{INK4a}$/pRb pathway, leading to senescence and concomitant expression of antifibrotic genes. Senescent fibroblasts accumulate in granulation tissues of healing cutaneous wounds and express antifibrotic genes in wild type mice. These processes are obliterated in knockin mice that express a senescence-defective CCN1 mutant, resulting in exacerbated fibrosis. Topical application of CCN1 protein to wounds reverses these defects. Thus, fibroblast senescence is a CCN1-dependent wound healing response in cutaneous injury, functioning to curb fibrosis during tissue repair.

INTRODUCTION

Originally characterized in human fibroblasts experiencing replicative exhaustion in culture[1], cellular senescence is an essentially irreversible form of cell-cycle arrest that can be triggered by a variety of cellular damages or stresses, including DNA damage, oncogene activation, oxidative stress, and telomere erosion[2],[3]. Senescent cells remain viable and metabolically active, but are unable to proliferate despite the presence of nutrients and mitogens. Recent studies have established cellular senescence as an important mechanism of tumor suppression by blocking the proliferation of damaged cells that may be at risk of neoplastic transformation[4]–[6]. However, senescent cells are also found in various noncancerous pathologies and aged tissues, although their roles in these contexts have not been thoroughly explored.

*Corresponding author: Department of Biochemistry and Molecular Genetics, University of Illinois at Chicago College of Medicine, Chicago, IL 60607. Tel: 312-996-6978; Fax: 312-996-7034. LFLau@uic.edu.

AUTHOR CONTRIBUTIONS J.-I.J. conducted the experiments; J.-I.J. and L.F.L. designed the experimental plan, analyzed the data, and wrote the paper.

COMPETING FINANCIAL INTERESTS The authors declare no competing financial interests.

In addition to cell-cycle arrest, senescent cells exhibit an enlarged and flattened cell morphology, accumulate senescence-associated β-galactosidase (SA-β-gal), and upregulate a number of secreted proteins that comprise the senescence-associated secretory phenotype (SASP) or the senescence messaging secretome (SMS)[2,7,8]. Proteins secreted by senescent cells include proinflammatory cytokines, growth regulatory factors, and participants in extracellular matrix (ECM) metabolism. Some of these secreted proteins, including IL-6, CXCR2 ligands, IGFBPs, and PAI-1, can reinforce or exacerbate senescence[9–13]. Although senescence can suppress tumorigenesis, some of the proteins secreted by senescent cells may paradoxically promote the malignant phenotypes of neighboring cells and disrupt the integrity and function of normal tissues[14], suggesting that the SASP/SMS may play diverse and context-dependent roles in tissue pathologies. Recent studies showed that senescent hepatic stellate cells accumulate in carbon tetrachloride (CCl_4)-induced liver damage and dampen liver fibrosis through the expression of antifibrotic proteins[15]. These results suggested that senescent cells may arise to limit fibrosis during tissue repair, although this possibility has not been examined beyond CCl_4-induced liver injury[15–17].

Among the proteins whose expression is associated with wound repair is the matricellular cell adhesive protein CCN1 (also known as CYR61), which regulates diverse cellular functions including cell adhesion, migration, differentiation, and survival in a cell type- and context-dependent manner[18]. CCN1 is a potent inducer of angiogenesis and *Ccn1*-null mice are embryonic lethal due to defects in cardiovascular development[19–21]. Here we show that CCN1, which is highly expressed in granulation tissues during cutaneous wound healing[22], drives fibroblasts into senescence and upregulates the expression of antifibrotic genes to restrict fibrosis during tissue repair. These findings uncover a pathway of senescence induction through integrin-mediated cell adhesion, and further establish senescence as a mechanism for controlling fibrogenesis in wound healing.

RESULTS

Accumulation of senescent cells in granulation tissue of healing wounds requires CCN1

Cutaneous wound healing occurs in three overlapping phases, initiating with an inflammatory phase marked by infiltration of neutrophils and macrophages, followed by a proliferative phase that includes ECM deposition, and a maturation phase that brings about matrix remodeling and resolution of the granulation tissue (Fig. 1a)[23,24]. CCN1 functions in fibroblasts are largely mediated through its direct binding to integrin $\alpha_6\beta_1$ and cell surface heparan sulfate proteoglycans (HSPGs)[25–29], whereas its angiogenic activities are mediated through integrin $\alpha_v\beta_3$[30]. Since *Ccn1*-null mice are embryonic lethal, to investigate the role of CCN1 in wound healing we have used knockin mice ($Ccn1^{dm/dm}$) in which the *Ccn1* genomic locus is replaced by an allele encoding DM, a CCN1 mutant with the $\alpha_6\beta_1$-HSPG binding sites disrupted by alanine substitutions[28]. Comparable levels of CCN1 protein were detected in full-thickness excisional wounds of wild type (WT; $Ccn1^{WT/WT}$) and $Ccn1^{dm/dm}$ mice, accumulating 5–9 days post-wounding[22] (Supplementary information, Fig. S1a). Although wounds of both genotypes healed completely by day 13, wound closure occurred with somewhat faster kinetics in $Ccn1^{dm/dm}$ mice (Fig. 1b). Consistent with faster healing, granulation tissue of $Ccn1^{dm/dm}$ mice showed a higher percentage of Ki-67-positive

proliferating cells than WT mice, whereas the numbers of apoptotic cells were essentially identical (Fig. 1c–d). These results indicated that proportionately more cells in WT wounds were driven out of the cell cycle in an apopotosis-independent manner, suggesting that some of these cells might be undergoing senescence.

Remarkably, granulation tissues of WT mice accumulated senescent cells as judged by SA-β-gal activity, most significantly between 7–9 days post-wounding when CCN1 expression peaked (Fig. 1e; Supplementary information, Fig. S1b). Although senescent cells have been isolated from human patients with chronic non-healing wounds[31],[32], to our knowledge they have not been previously reported in models of normal cutaneous wounds. SA-β-gal-positive cells were virtually abolished in granulation tissue of *Ccn1*$^{dm/dm}$ mice, indicating that CCN1 is critical for the establishment or maintenance of cellular senescence. Furthermore, the senescence markers p16^{INK4a} and p53 were detected in WT but not in *Ccn1*$^{dm/dm}$ wounds (Fig. 1f; Supplementary information, Fig. S1c). Cells staining positive for p16^{INK4a} or p53 were also positive for α-smooth muscle actin (α-SMA), indicating that the senescent cells were myofibroblasts. To verify these results, fibroblasts were isolated from 7- and 9-day wounds and plated in tissue culture dishes; ~11–15 % of cells from WT wounds were SA-β-gal-positive, compared to ~3% from *Ccn1*$^{dm/dm}$ mice (Fig. 1g). These results show that CCN1, acting through its $\alpha_6\beta_1$-HSPG binding sites, is required for the accumulation of senescent fibroblasts in granulation tissue during cutaneous wound healing.

CCN1 induces senescence in human fibroblasts through integrin signaling

To test whether CCN1 can directly induce cellular senescence, we treated young human BJ skin fibroblasts cultured in 10% serum with purified recombinant CCN1 protein. We found that CCN1 induced premature senescence as judged by several criteria. First, CCN1 arrested cell proliferation within 3 days, as shown by stagnant cell numbers and >50% decrease in BrdU incorporation and Ki-67 index compared to BSA-treated controls (Fig. 2a–c), whereas no apoptosis was observed with or without CCN1 (data not shown). CCN1 inhibited cell proliferation in a dose-dependent manner, detectable at 250 ng/ml and maximal at 5 μg/ml (Supplementary information, Fig. S2a). Second, CCN1-induced growth arrest was irreversible once established, even after CCN1 was removed. Cells treated with CCN1 for 6 days to establish senescence were harvested by trypsinization and replated in fresh medium to remove extracellular CCN1. The replated cells did not divide further even after 6 more days of culture in the absence of CCN1 (Fig. 2d). Third, CCN1-treated fibroblasts exhibited an enlarged and flattened cell morphology characteristic of senescent cells (Fig. 2e), and fourth, these cells expressed markers of senescence including SA-β-gal, p53 and p16^{INK4a} (Fig. 2f–h). Consistent with the SASP/SMS, CCN1-treated cells upregulated the expression of several proinflammatory cytokines (*IL6, IL8, IL11*) and matrix degrading enzymes (*MMP1, MMP3*), and significantly downregulated expression of type I collagen (*COL1A1*; Fig. 2i–k). CCN1 also induced senescence phenotypes in IMR-90 human diploid lung fibroblasts, indicating that this response is not limited to BJ cells (Supplementary information, Fig. S2b–c).

Since CCN1 is an ECM cell adhesion molecule, we tested its activity as a cell adhesion substrate. BJ cells expressed SA-β-gal when plated on immobilized CCN1 but not on

fibronectin (FN), laminin (LN), or vitronectin (VN; Fig. 3a), indicating that CCN1 can induce senescence as a cell adhesion substrate and this activity is unique among the ECM proteins tested. Consistent with impaired senescence in *Ccn1*$^{dm/dm}$ mice, purified DM protein[26] was completely unable to inhibit DNA synthesis, induce SA-β-gal expression, or trigger the SASP/SMS (Fig. 3b–d; Supplementary information, Fig. S2e). By contrast, D125A[30], a single amino acid substitution CCN1 mutant defective for binding α_v integrins, was unaffected in its senescence-inducing activities (Fig. 3b–d). Pretreatment of cells with either function-blocking monoclonal antibody (mAb) against α_6 integrin or addition of soluble heparin inhibited CCN1-induced SA-β-gal expression, whereas mAb against $\alpha_v\beta_3$ had no effect, indicating the involvement of $\alpha_6\beta_1$ and HSPGs (Fig. 3e,g). Furthermore, the addition of an $\alpha_6\beta_1$-specific binding peptide (T1)[33] as competitor blocked CCN1-induced senescence, whereas the peptide with a two-residue substitution (T1-mut) that abrogated $\alpha_6\beta_1$ binding was ineffective (Fig. 3f). These results indicate that CCN1 induces senescence through an integrin-mediated mechanism involving $\alpha_6\beta_1$ and HSPGs.

CCN1-induced senescence requires participation of both p53 and p16^{INK4a}

Cellular responses to known senescence-inducing signals are established and maintained by either the p53 or p16^{INK4a}/pRb tumor suppressor pathway, or both, depending on the cell type and context[2,3]. Both p53 and p16^{INK4a} proteins accumulated upon CCN1 treatment, indicating their activation (Fig. 4a). It is known that DNA damage response (DDR) induced by double strand breaks or uncapped telomeres can result in activation of ATM and Chk2; phosphorylation of p53 by Chk1 or Chk2 at Ser-20 stabilizes p53 by dissociating it from HDM2/Mdm2[34,35]. CCN1 induced phosphorylation of ATM, Chk1, and Chk2, and concomitantly, phosphorylation of p53 on Ser-20 (Fig. 4b), indicating that CCN1 activates DDR and p53. p53 can also be activated by other forms of cellular stress, including ROS[36]. CCN1 activation of p53 was partially inhibited by the ROS scavenger *N*-acetyl cysteine (NAC), indicating that CCN1 activates p53 in part through a ROS-dependent pathway (Supplementary Information Fig. S3a). pRb was also activated by CCN1 as judged by its hypophosphorylation concomitant with the induction of p16^{INK4a}, which can activate pRb independent of p53 by inhibiting Cdk4 and Cdk6. To interrogate the functional role of p53, we expressed short hairpin RNAs (shRNAs) to silence its expression. Complete p53 knockdown using two different shRNA sequences (shp53#1 and #3) restored cell proliferation by ~80%, whereas a partial knockdown (shp53#2) achieved an intermediate effect (Fig. 4c–d). Expression of shRNAs *per se* did not affect cell growth (Fig. 4d,f). Likewise, silencing of p16^{INK4a} by either expression of shRNA (shp16^{INK4a}) or its suppressor *Bmi-1*[37] partially restored CCN1-induced growth suppression by <60% (Fig. 4e–f). These results show that the p53 and p16^{INK4a}/pRb pathways both contribute to CCN1-induced senescence.

CCN1 induces senescence through $\alpha_6\beta_1$-dependent ROS generation via activation of NOX1

Since CCN1 is known to induce ROS accumulation[28,29], which can induce senescence[36,38], we assessed the role of ROS. Pretreatment of cells with NAC abrogated CCN1-induced senescence (Fig. 5a–b), indicating the requirement of ROS. CCN1-induced ROS accumulation was mediated through $\alpha_6\beta_1$, as it was obliterated in cells pre-treated with anti-

α_6 mAb but not with anti-$\alpha_v\beta_3$ mAb (Fig. 5c). Since cell adhesion can generate ROS[39], we compared ROS accumulation upon cell adhesion to CCN1 and other ECM proteins to assess how CCN1 uniquely triggers senescence. Cell adhesion to FN, LN, VN and type I collagen (Col. I) transiently induced a low level of ROS that returned to background levels by 4 hrs in most cases, whereas cell adhesion to CCN1 induced a higher level of ROS that was sustained for at least 4 hrs (Fig. 5d). Moreover, addition of NAC 3–6 h post-CCN1 treatment completely blocked senescence, whereas NAC added 10 and 24 h post-CCN1 treatment was partially and completely ineffective, respectively (Fig. 5e). Thus, CCN1 induces a high level of ROS, which must be sustained for least 6–10 hrs for the establishment of senescence.

NADPH oxidases (NOXs) and 5-lipoxygenase (5-LOX) participate in ROS generation downstream of ECM-integrin interactions[28,39]. The NOX inhibitor apocynin blocked CCN1-induced senescence whereas the 5-LOX inhibitor MK886 did not, suggesting that NOX, but not 5-LOX, might be responsible for ROS necessary for senescence (Fig. 6a). Consistently, shRNAs (sh5LOX #2) that completely silenced 5-LOX expression had no effect on CCN1-induced proliferation arrest (Fig. 6b). Among the five NOX isoforms, NOX1 and NOX4 are widely expressed in non-phagocytic cells including fibroblasts[40]. CCN1 upregulated *NOX1* expression in BJ cells whereas *NOX4* and catalase expression was unaffected (Fig. 6c), suggesting that NOX1 may be critical. Knockdown of NOX1 by either of two shRNAs (#1 and #2) partially bypassed CCN1-induced growth arrest, whereas knockdown of NOX4 had no effect (Fig. 6d). Furthermore, RAC1 is required for NOX1 activation, especially when cellular levels of co-activating proteins NOXO1 and NOXA1 are low, but is dispensable for NOX4 activity[40]. RAC1 is known to be activated by CCN1-induced adhesive signaling through $\alpha_6\beta_1$-HSPGs[41]. Depletion of RAC1 by shRNA rescued cells from CCN1-induced growth arrest, consistent with the requirement for NOX1 (Fig. 6e). Thus, CCN1 induces the expression of NOX1 and its activation through RAC1, thereby activating the superoxide-generating RAC1-NOX1 complex required for CCN1-induced senescence. Consistently, the accumulation of superoxides in healing wounds is blunted in *Ccn1*$^{dm/dm}$ mice, indicating its dependence on CCN1 (Supplementary information, Fig. S3b).

Induction of p16^{INK4a} through ROS-dependent activation of ERK and p38MAPK

The induction of p16^{INK4a} is regulated by mitogenic and stress-response pathways, including the extracellular signal regulated kinase (ERK; p42/p44) and p38 mitogen-activated protein kinase (MAPK)[42,43]. Both ERK and p38 MAPK, but not JNK, were activated by phosphorylation in a biphasic manner upon CCN1 treatment (Fig. 7a; Supplementary information, Fig. S3d). The first activation phase occurred within 3 hrs after CCN1 treatment, followed by inactivation and reactivation in the second phase by 24 hrs. Pretreatment of cells with inhibitors of p38 MAPK (SB202190) or the ERK activating kinase MEK1 (PD98059) blocked CCN1-induced SA-β-gal expression, whereas the JNK inhibitor SP600126 had little effect (Fig. 7b). Moreover, both SB202190 and PD98059 abrogated CCN1-induced p16^{INK4a} expression, but SP600126 had no effect (Fig. 7c and data not shown). These results show that ERK and p38 MAPK, but not JNK, are required for CCN1-mediated induction of p16^{INK4a}, which is critical for senescence.

ROS can activate stress-activated kinases such as MAPKs through activation of the redox-sensitive ASK1[44], and sustain MAPK activation by neutralizing MAPK phosphatases via oxidative inactivation of the cysteine residue at their active sites[45]. Therefore, we tested whether CCN1-induced ERK and p38 MAPK activation may be ROS-dependent (Fig. 7d). Both kinases were activated by CCN1 in a biphasic manner (3h and 24h), and apocynin effectively abrogated ERK and p38 MAPK activation at both early and late phases. NAC also blocked ERK activation at both time points, and inhibited late activation of p38 MAPK. Together, these results show that CCN1-induced ROS generation leads to the activation of ERK and p38 MAPK, triggering $p16^{INK4a}$ induction and cellular senescence (Fig. 7e).

CCN1-regulated senescence restricts fibrosis in cutaneous wound healing

The fibrogenic response contributes to tissue repair by helping to reconstitute the damaged tissue through ECM deposition, although excessive fibrosis may impair tissue function[24,46]. Senescent cells express an antifibrotic genetic program and may thus protect against excessive fibrosis during wound healing[2,15]. To test whether CCN1-induced senescence regulates fibrosis *in vivo*, we quantified the expression of genes relevant to fibrosis in wound tissues. Granulation tissue of WT mice expressed much higher levels of *Mmp2*, *Mmp3*, and *Mmp9* than $Ccn1^{dm/dm}$ mice (Fig. 8a). $Ccn1^{dm/dm}$ wounds lacked senescent cell accumulation and expressed a higher level of *Col1a1* and the fibrotic mediator *Tgfb1*, indicating an enhanced fibrotic response (Figs. 1e, 8b). Actual collagen deposition as measured by hydroxyproline content was significantly higher in $Ccn1^{dm/dm}$ wounds, a difference that persisted at least 21 days post-wounding, well passed the completion of wound closure (Fig. 8c). Staining of granulation tissues with Sirius red revealed a substantial increase in collagen in $Ccn1^{dm/dm}$ wounds under polarized light (Fig. 8d–e). To assess the role of CCN1 in wound healing directly, we treated excisional cutaneous wounds in $Ccn1^{dm/dm}$ mice with topical applications of purified CCN1 protein or buffered saline. Addition of CCN1 reversed the profibrotic phenotype of $Ccn1^{dm/dm}$ mice, resulting in significantly enhanced expression of *Mmp2*, *Mmp3*, and *Mmp9*, reduced expression of *Col1a1* and *Tgfb1*, and curtailed collagen deposition as detected by Sirius red staining (Fig. 8f–g). Furthermore, application of CCN1 protein induced cellular senescence in cutaneous wounds in the senescence-deficient $Ccn1^{dm/dm}$ mice (Fig. 8h). Together, these results show that CCN1 induces cellular senescence in granulation tissue and curbs the fibrogenic response during cutaneous wound healing.

DISCUSSION

We show here that the matricellular protein CCN1 induces fibroblast senescence through an integrin-mediated mechanism, resulting in the expression of antifibrotic genes to dampen fibrosis in cutaneous wound healing. Rapid synthesis of ECM occurs in wound repair to provide structural integrity to damaged tissues, although excessive matrix deposition can lead to fibrosis and scarring where ECM replaces parenchyma, resulting in loss of tissue function[24,46]. Fibrosis commonly occurs as a result of persistent wound healing response to chronic injuries in many mammalian organs, for example in the liver in response to viral infections, alcoholism, and non-alcoholic fatty liver disease, in the lung due to cigarette smoking, and in the heart after myocardial infarctions[23,46]. Since the wound healing process

in most mammalian organs are remarkably similar irrespective of the underlying etiology[24], our findings in cutaneous wound healing may be informative to wound repair more generally. Indeed, our findings echo those of recent studies showing that senescent hepatic stellate cells accumulate in CCl_4-induced liver injury to limit fibrosis[15]. These and our findings support the notion that cellular senescence may occur as a general, programmed wound healing response that functions in disparate organ systems to control fibrosis. Therefore, whereas cellular senescence has an established role in tumor suppression, its contribution to the biology of wound healing and tissue repair is beginning to emerge.

Ccn1 was first identified as an immediate-early gene inducible by serum growth factors in fibroblasts[47]. Although serum was initially thought to induce a genetic program for cell proliferation, later genomic analyses indicated that a subset of serum-inducible genes represented a wound healing response[48]. Consistently, *Ccn1* is highly expressed at sites of wound healing in various tissues, including cutaneous, cardiovascular, and bone injuries[18]. Here we provide direct evidence that CCN1 plays critical roles in cutaneous wound healing by its induction of fibroblast senescence and expression of antifibrotic genes. Topical treatment of wounds with purified CCN1 reversed the enhanced fibrogenesis suffered by mice lacking senescence-competent CCN1 (Fig. 8). These findings establish the functions of CCN1 in cutaneous wounds, and suggest that exogenous delivery of CCN1 or induction of CCN1 signaling may have therapeutic value for the treatment of fibrosis associated with wound healing. The specific triggers that activate CCN1 expression during wound healing are as yet unknown, although the *Ccn1* promoter is responsive to a wide spectrum of inducing signals[47],[49]. Interestingly, a related member of the CCN family, *Ccn2*, mediates profibrotic responses in diverse pathologies[50],[51]. Thus, CCN1 and CCN2 may regulate the fibrogenic process during wound healing in disparate and possibly opposing ways.

CCN1 induces cellular senescence by binding to its cell adhesion receptors, integrin $\alpha_6\beta_1$ and cell surface HSPGs, to engage both p53- and $p16^{INK4a}$-dependent senescence pathways. Mice nullizygous for *p53* and *INK4a/ARF* are deficient in senescent cell accumulation in CCl_4-induced liver injury[15], suggesting that cellular senescence may occur through similar pathways in diverse models of wound healing. Mechanistically, CCN1 triggers senescence by activating p53 through induction of a DDR and in part through a ROS-dependent pathway (Figs. 4b; Supplementary Information, Fig. S3a). CCN1 also induces ROS generation through the RAC1-NOX1 complex and ROS-dependent biphasic activation of ERK and p38 MAPK, leading to induction of the $p16^{INK4a}$/pRb pathway (Fig. 7e). Although the cell adhesion process generates ROS, CCN1 is unique among ECM proteins as a cell adhesive substrate in triggering a robust and sustained accumulation of ROS necessary for senescence. Whereas CCN1 can induce ROS generation through multiple mechanisms[28],[29], distinct cellular sources of ROS may participate in disparate biological functions with specificity. For example, apoptotic synergism between CCN1 and TNFα requires ROS generated through 5-LOX but not NOX[28], whereas CCN1-induced senescence requires NOX1 but not 5-LOX (Fig. 6). The specific nature, kinetics, and/or subcellular localization of ROS generated by distinct cellular sources may contribute to their functional specificity[52].

Whether CCN1 is required for cellular senescence in disparate organ systems and in broader biological contexts beyond wound repair is currently unknown. However, it is noteworthy that CCN1 expression is elevated in several human pathologies associated with the occurrence of senescent cells, including atherosclerotic plaques, benign prostatic hyperplasia, and chronologically aged human skin[53–56]. These results suggest that CCN1 may contribute to senescence in certain age-related diseases and conditions. Both cellular senescence and apoptosis function in tumor suppression[2,17], and CCN1 can synergize with TNFα and related cytokines to trigger robust apoptosis *in vitro* and *in vivo*[28,29,57], suggesting that CCN1 may function as a tumor suppressor by inducing apoptosis and/or senescence. Indeed, several studies have suggested that CCN1 may suppress tumorigenesis[58–61]. Paradoxically, CCN1 is also a potent angiogenic inducer and may promote tumor growth[18,19]. Thus, the role of CCN1 in tumorigenesis may be cell type- and context-dependent, and may hinge upon whether angiogenic factors are limiting or whether conditions conducive for apoptosis or senescence prevail. Defining the roles of CCN1-induced senescence in diverse models of wound healing, aging-related pathologies, and tumorigenesis clearly merits further investigation.

METHODS

Cell culture

Human BJ foreskin fibroblasts (ATCC# CRL-2522) and IMR-90 lung fibroblasts (ATCC# CCL-186) were maintained at 37 °C in 5% CO_2 in Eagle's minimum essential medium (EMEM) containing 10% FBS (Hyclone), 1% penicillin/streptomycin, non-essential amino acids and sodium pyruvate. The cumulative population doubling (CPD) was calculated using the formula $n = (\log_{10} F - \log_{10} I)/\log 2$, where F is the number of cells at the end of one passage, I is the number of cells that were seeded at the beginning of one passage, and is the number of population doublings occurring in that passage. BJ cells were used between PD30 to PD45.

CCN1 proteins and reagents

Recombinant CCN1 and mutant proteins (D125A and DM) were produced using a baculovirus expression system in insect cells and purified by ion-exchange or immuno-affinity chromatography[22, 26]. Human FN, VN, mouse LN, rat tail Col.I were from BD Biosciences. Poly-L-Lysine (PLL), heparin sodium salt, and rabbit and mouse IgGs were from Sigma. Apocynin, MK886, PD98059, SB202190, SP600126, and function-blocking mAb against integrins α_6 (GoH3) and $\alpha_V\beta_3$ (LM609) were from Chemicon. The synthetic peptides T1 (GQKCIVQTTSWSQCSKS) and T1-mut (GQKCIVQTTSAAQCSKS) were previously described[27, 33]. HRP-conjugated anti-mouse and anti-rabbit secondary antibodies were from Amersham. Biotin-conjugated goat anti-rabbit IgG antibody and streptavidin-conjugated HRP were from Invitrogen.

Analysis of cell proliferation and senescence

SA-β-gal assay was performed as described[62]. For analysis in wounds, frozen tissue sections (6 μm) were fixed in 1% formalin before staining, and counterstained with Eosin. For growth curves, cells (1×10^4 cells per well) were grown in 12-well plates and treated as

indicated. Cells were stained with 1% trypan blue (Invitrogen) and the total cell numbers counted. For BrdU incorporation and Ki-67 immunostaining, cells in 8-well chamber slides (2×10^3 cells per well) were treated with CCN1 for 3 days and either left untreated or labeled with BrdU (10 μg/ml, Roche applied science) for 2h. Then cells were fixed using Carnoy's fixative (ethanol:acetic acid=3:1), washed, and BrdU-/Ki-67 positive cells were visualized by FITC-conjugated anti-BrdU Ab (Millipore) or TRITC-conjugated anti-Ki67 Ab (Abcam), respectively. Fluorescence images were taken from 5 random fields in each well using a Zeiss Axiovert 200 M microscope with the AxioCam MRc5 camera (AxioVision Rel 4.6 software) and BrdU/Ki-67 positive cells were scored and normalized against DAPI positive cells. All assays were done in triplicates, and ~300 cells were counted in each sample from randomly selected fields.

Western blot analysis

Western blot analyses were performed using standard procedure with chemiluminescence using ECL system (GE Heathcare). Antibodies against the following proteins were used: p53 (DO-1; SC126) and p16 (H-156; SC756) from SantaCruz Biotech; p-ERK1/2 (Thr202/Tyr204; #9101), ERK1/2 (137F5; #4695), p-p38MAPK (Thr180/Tyr182; 28B10; #9216), p38MAPK (#9212), p-JNK1/2 (Thr183/Tyr185; #9251), JNK1/2 (#9252), p-Chk1 (S345; #2341), p-Chk2 (Thr68; #2661), p-p53 (Ser20; #9287) from Cell Signaling; RAC1 (#07-1464) from Millipore; p-ATM (Ser-1981; #200-301-400) from Rockland; Rb (G3-245; 554136) from BD Pharmingen; 5-Lipoxygenase (Ab59341) from Abcam; and β-actin (AC-15) from Sigma.

RNAi and lentiviral infection

For RNA interference, 19-nucleotide target sequences were designed using software of the RNAi consortium (BROAD institute) and cloned into the *Mlu* I and *Cla* I sites of the pLVTHM vector (Addgene; 12247), where the TTCAAGAGA loop sequence links the 19-nt sense and antisenence sequences. Target sequences for each molecule are described in Supplementary Information, Table I. For lentiviral supernatants production, 293FT cells (Invitrogen) were transfected using the $CaCl_2$ method with the following transfer plasmids: pLVTHM, pshp53 (#1, #2 and #3)[63–65], pBmi1 (Addgene; 12240), pSINpuro-sip16 (a generous gift from Dr. Scott W. Lowe)[66], pshNOX1 (#1 and #2), pshNOX4, psh5LOX (#1 and #2), and pshRAC1 using either 2nd or 3rd generation packaging system. After 48 to 72 h, the viral supernatants were collected through 0.45 μm filter and stored at −80 °C. For infection, cells were plated (3×10^5 cells per 60 mm dish) and infected with a cocktail (3:1 ratio of growth media to viral supernatant) containing 1.5 μg/ml polybrene for 48h. Cells were then re-plated as each experiment required. The infection efficiency (>99%) was determined by monitoring expression of green fluorescent protein encoded by the pLVTHM vector.

RNA isolation and semiquantitative RT-PCR/qRT-PCR

BJ cells or skin wound tissues were homogenized using TRIzol reagent (Invitrogen) and total RNA from each sample was isolated using RNeasy® Mini Kit (Quiagen). Total RNA (2 μg) were reverse transcribed to cDNA using MMLV-Reverse Transcriptase (Promega),

and qRT-PCR was performed with the iCycler Thermal Cycler (Bio-Rad) using iQ SYBR Green Supermix (Bio-Rad). The specificity of qRT-PCR was confirmed by agarose gel electrophoresis and melting-curve analysis. A housekeeping gene (β-actin or cyclophilinE) was used as an internal standard. The primers used in this study are described in Supplementary information, Table II.

ROS and superoxide measurements

H_2DCF-DA (Invitrogen) for H_2O_2 and dihydroethidium (DHE; Invitrogen) for O^{2-} were used for ROS measurement as described[28]. Briefly, cells were plated on 8-well chamber slides or slides pre-coated with matrix proteins and treated with CCN1 for indicated times. Cells were then incubated with either H_2DCF-DA or DHE (10 μM, each) for 10 min at 37 °C, washed with 0.5% BSA containing HANKS' balanced salt solution (HBSS). The fluorescence images were acquired using Leica DM IRB microscope and fluorescence intensity was calculated using ImageJ software (NIH). For measurement in tissues, cutaneous wounds were harvested various days after wounding and superoxide levels were quantified by lucigenin-enhanced chemi-luminescence[67]. Skin tissues were cut into small pieces (2×2 mm) and placed in polypropylene tubes containing 5 μmol/L lucigenin in 1 mL modified Krebs' solution. Tubes were read in a luminometer (TD-20, Turner Designs). The luminometer reports relative light units emitted, which were integrated over 5 min. After measurement, tissues were dried overnight and dry weight was measured.

Animals and cutaneous wound healing

Animal protocols were approved by the Institutional Animal Care and Use Committee of the University of Illinois at Chicago. Two independent lines of *Ccn1*$^{dm/dm}$ mice were generated in a svJ129-C57BL/6 mixed background[28] and backcrossed a minimum of 10 times into the C57BL/6 background. *Ccn1*$^{WT/WT}$ *and Ccn1*$^{dm/dm}$ mice (12 weeks of age) were anesthetized with intraperitoneal (IP) injection of ketamine/xylazine (100 mg/kg IP) and the dorsum of each mouse was clipped free of hair. Full-thickness excisional wounds were created with a 6 mm biopsy punch (Miltex) and left open during the healing process. Wound sizes were measured daily. Mice were sacrificed at 5, 7, 9, 13 and 21 days post-wounding and wound tissues harvested. Wound tissues were snap-frozen in O.C.T. compound (Tissue-Tek) and sectioned serially (6 μm thickness) using a Leica CM1950 UV cryostat. Anti-Ki67 polyclonal antibody was used for monitoring proliferation in the granulation tissues and a biotinylated goat anti-rabbit secondary antibody is coupled with streptavidin-horseradish peroxidase (HRP), followed by the reaction with 3,3'-Diaminobenzidine (DAB; Sigma) to produce brown nuclear staining. Sections were counterstained with hematoxylin. Apoptosis during wound healing was detected by TUNEL assay using ApopTag Red *in situ* apoptosis detection kit (Millipore) and visualized under the fluorescence microscopy (Zeiss; Axiovert 200M).

Topical CCN1 treatment during wound healing

Recombinant CCN1 protein was diluted in PBS to a concentration of 0.1 μg/μl, and 50 μl of protein or saline control was directly applied daily to each full-thickness excisional wound

created in *Ccn1*$^{dm/dm}$ mice. Wound tissues were collected 9 days post-wounding and processed for analysis.

Immunofluorescence

Frozen wound tissues were processed for double immunofluorescence. Acetone-fixed wound tissue sections were washed in PBST (2×) for 2 min and incubated in normal goat serum blocking solution containing 2% goat serum, 1% BSA, 0.1% cold fish skin gelatin, 0.1% Triton X-100, 0.05% Tween 20, 0.05% sodium azide, and 0.01M PBS (pH 7.2) for 1h. For labeling, the antibody mix containing either anti-p16 polyclonal antibody (M156, SantaCruz) and anti-smooth muscle actin mAb (Sigma) or anti-p53 mAb (DO-1; SantaCruz) and anti-smooth muscle actin polyclonal antibody (Abcam) was applied for 2 h at room temperature. After washing (5×) in PBST, the slides were incubated with the secondary antibody mix (TRITC-conjugated anti-mouse IgG and FITC-conjugated anti-rabbit IgG for p53, TRITC-conjugated anti-rabbit IgG and FITC-conjugated anti-mouse IgG for p16) for 30 min, followed by washing (5×) in PBST. For counterstaining, DAPI (1 μg/ml) was used. The fluorescence images were acquired using with a Zeiss Axiovert 200 M microscope and processed with Photoshop 7 (Adobe).

Isolation of cells from wounds and measurement of collagen deposition in wounds

Cells were isolated from 7- and 9-day wounds (n=3) as described[68] and plated in 60 mm culture dishes. For hydrxoyproline assay, skin wounds (n=3 for both genotypes) were harvested at indicated days and dried in 110°C oven overnight, placed in a screw-capped glass vessel and hydrolyzed in 6 *N* hydrochloric acid at 110°C for 18 h. The lysates were processed and hydroxyproline content determined as described[69], using purified hydroxyproline to generate a standard curve. Alternatively, frozen section of wound tissues were processed for Sirius red staining (Sigma) and viewed under polarized light. The Sirius red-positive area was calculated using ImageJ software (NIH).

Statistics

Results are expressed as the mean ± S.D., and statistical analysis was performed by one-way ANOVA analysis of variance and Student's *t*-test. A $p<0.05$ was considered significant.

Supplementary Material

Refer to Web version on PubMed Central for supplementary material.

ACKNOWEDGEMENTS

We thank Dr. Luisa DiPietro for invaluable expert advice, Drs. Judith Campisi and Scott Lowe for generous gifts of reagents, Seung Won Shin for excellent assistance, and members of the laboratory for helpful discussion. This work was supported by grants from the National Institutes of Health (GM78492 and CA46565) to L.F.L.

Reference List

1. Hayflick L. The limited in vitro lifetime of human diploid cell strains. Exp. Cell Res. 1965; 37:614–636. [PubMed: 14315085]

2. Campisi J, d'Adda di Fagagna F. Cellular senescence: when bad things happen to good cells. Nat. Rev. Mol. Cell Biol. 2007; 8:729–740. [PubMed: 17667954]
3. Collado M, Blasco MA, Serrano M. Cellular senescence in cancer and aging. Cell. 2007; 130:223–233. [PubMed: 17662938]
4. Braig M, et al. Oncogene-induced senescence as an initial barrier in lymphoma development. Nature. 2005; 436:660–665. [PubMed: 16079837]
5. Chen Z, et al. Crucial role of p53-dependent cellular senescence in suppression of Pten-deficient tumorigenesis. Nature. 2005; 436:725–730. [PubMed: 16079851]
6. Michaloglou C, et al. BRAFE600-associated senescence-like cell cycle arrest of human naevi. Nature. 2005; 436:720–724. [PubMed: 16079850]
7. Kuilman T, Peeper DS. Senescence-messaging secretome: SMS-ing cellular stress. Nat. Rev. Cancer. 2009; 9:81–94. [PubMed: 19132009]
8. Young AR, Narita M. SASP reflects senescence. EMBO Rep. 2009; 10:228–230. [PubMed: 19218920]
9. Kortlever RM, Higgins PJ, Bernards R. Plasminogen activator inhibitor-1 is a critical downstream target of p53 in the induction of replicative senescence. Nat. Cell Biol. 2006; 8:877–884. [PubMed: 16862142]
10. Kuilman T, et al. Oncogene-induced senescence relayed by an interleukin-dependent inflammatory network. Cell. 2008; 133:1019–1031. [PubMed: 18555778]
11. Acosta JC, et al. Chemokine signaling via the CXCR2 receptor reinforces senescence. Cell. 2008; 133:1006–1018. [PubMed: 18555777]
12. Wajapeyee N, Serra RW, Zhu X, Mahalingam M, Green MR. Oncogenic BRAF induces senescence and apoptosis through pathways mediated by the secreted protein IGFBP7. Cell. 2008; 132:363–374. [PubMed: 18267069]
13. Augert A, et al. The M-type receptor PLA2R regulates senescence through the p53 pathway. EMBO Rep. 2009; 10:271–277. [PubMed: 19197340]
14. Coppe JP, et al. Senescence-associated secretory phenotypes reveal cell-nonautonomous functions of oncogenic RAS and the p53 tumor suppressor. PLoS. Biol. 2008; 6:2853–2868. [PubMed: 19053174]
15. Krizhanovsky V, et al. Senescence of activated stellate cells limits liver fibrosis. Cell. 2008; 134:657–667. [PubMed: 18724938]
16. Adams PD. Healing and Hurting: Molecular Mechanisms, Functions, and Pathologies of Cellular Senescence. Mol. Cell. 2009; 36:2–14. [PubMed: 19818705]
17. Evan GI, d'Adda di Fagagna F. Cellular senescence: hot or what? Curr. Opin. Genet. Dev. 2009; 19:25–31. [PubMed: 19181515]
18. Chen C-C, Lau LF. Functions and Mechanisms of Action of CCN Matricellular Proteins. Int. J. Biochem. Cell Biol. 2009; 41:771–783. [PubMed: 18775791]
19. Babic AM, Kireeva ML, Kolesnikova TV, Lau LF. CYR61, product of a growth factor-inducible immediate-early gene, promotes angiogenesis and tumor growth. Proc. Natl. Acad. Sci. U. S. A. 1998; 95:6355–6360. [PubMed: 9600969]
20. Mo FE, et al. CYR61 (CCN1) Is Essential for Placental Development and Vascular Integrity. Mol. Cell Biol. 2002; 22:8709–8720. [PubMed: 12446788]
21. Mo F-E, Lau LF. The matricellular protein CCN1 is essential for cardiac development. Circ. Res. 2006; 99:961–969. [PubMed: 17023674]
22. Chen C-C, Mo F-E, Lau LF. The angiogenic inducer Cyr61 induces a genetic program for wound healing in human skin fibroblasts. J. Biol. Chem. 2001; 276:47329–47337. [PubMed: 11584015]
23. Stramer BM, Mori R, Martin P. The inflammation-fibrosis link? A Jekyll and Hyde role for blood cells during wound repair. J. Invest Dermatol. 2007; 127:1009–1017. [PubMed: 17435786]
24. Gurtner GC, Werner S, Barrandon Y, Longaker MT. Wound repair and regeneration. Nature. 2008; 453:314–321. [PubMed: 18480812]
25. Chen N, Chen CC, Lau LF. Adhesion of human skin fibroblasts to Cyr61 is mediated through integrin α6β1 and cell surface heparan sulfate proteoglycans. J. Biol. Chem. 2000; 275:24953–24961. [PubMed: 10821835]

26. Leu S-J, et al. Targeted mutagenesis of the matricellular protein CCN1 (CYR61): selective inactivation of integrin α6β1-heparan sulfate proteoglycan coreceptor-mediated cellular activities. J. Biol. Chem. 2004; 279:44177–44187. [PubMed: 15322081]
27. Todorovic V, Chen C-C, Hay N, Lau LF. The matrix protein CCN1 (CYR61) induces apoptosis in fibroblasts. J. Cell Biol. 2005; 171:559–568. [PubMed: 16275757]
28. Chen C-C, et al. Cytotoxicity of TNFα is regulated by Integrin-Mediated Matrix Signaling. EMBO J. 2007; 26:1257–1267. [PubMed: 17318182]
29. Juric V, Chen CC, Lau LF. Fas-Mediated Apoptosis is Regulated by the Extracellular Matrix Protein CCN1 (CYR61) in vitro and in vivo. Mol. Cell Biol. 2009; 29:3266–3279. [PubMed: 19364818]
30. Chen N, Leu S-J, Todorovic V, Lam SCT, Lau LF. Identification of a novel integrin αvβ3 binding site in CCN1 (CYR61) critical for pro-angiogenic activities in vascular endothelial cells. J Biol. Chem. 2004; 279:44166–44176. [PubMed: 15308622]
31. Mendez MV, et al. Fibroblasts cultured from venous ulcers display cellular characteristics of senescence. J. Vasc. Surg. 1998; 28:876–883. [PubMed: 9808856]
32. Stanley A, Osler T. Senescence and the healing rates of venous ulcers. J. Vasc. Surg. 2001; 33:1206–1211. [PubMed: 11389419]
33. Leu S-J, et al. Identification of a novel integrin α6β1 binding site in the angiogenic Inducer CCN1 (CYR61). J. Biol. Chem. 2003; 278:33801–33808. [PubMed: 12826661]
34. Caspari T. How to activate p53. Curr. Biol. 2000; 10:R315–R317. [PubMed: 10801407]
35. Herbig U, Jobling WA, Chen BP, Chen DJ, Sedivy JM. Telomere shortening triggers senescence of human cells through a pathway involving ATM, p53, and p21(CIP1), but not p16(INK4a). Mol. Cell. 2004; 14:501–513. [PubMed: 15149599]
36. Catalano A, Rodilossi S, Caprari P, Coppola V, Procopio A. 5-Lipoxygenase regulates senescence-like growth arrest by promoting ROS-dependent p53 activation. EMBO J. 2005; 24:170–179. [PubMed: 15616590]
37. Jacobs JJ, Kieboom K, Marino S, DePinho RA, van LM. The oncogene and Polycomb-group gene bmi-1 regulates cell proliferation and senescence through the ink4a locus. Nature. 1999; 397:164–168. [PubMed: 9923679]
38. Lu T, Finkel T. Free radicals and senescence. Exp. Cell Res. 2008; 314:1918–1922. [PubMed: 18282568]
39. Chiarugi P. Reactive oxygen species as mediators of cell adhesion. Ital. J. Biochem. 2003; 52:28–32. [PubMed: 12833635]
40. Lambeth JD, Kawahara T, Diebold B. Regulation of Nox and Duox enzymatic activity and expression. Free Radic. Biol. Med. 2007; 43:319–331. [PubMed: 17602947]
41. Chen C-C, Chen N, Lau LF. The angiogenic factors Cyr61 and CTGF induce adhesive signaling in primary human skin fibroblasts. J. Biol. Chem. 2001; 276:10443–10452. [PubMed: 11120741]
42. Iwasa H, Han J, Ishikawa F. Mitogen-activated protein kinase p38 defines the common senescence-signalling pathway. Genes Cells. 2003; 8:131–144. [PubMed: 12581156]
43. Wen-Sheng W. ERK signaling pathway is involved in p15INK4b/p16INK4a expression and HepG2 growth inhibition triggered by TPA and Saikosaponin a. Oncogene. 2003; 22:955–963. [PubMed: 12592382]
44. Tobiume K, et al. ASK1 is required for sustained activations of JNK/p38 MAP kinases and apoptosis. EMBO Rep. 2001; 2:222–228. [PubMed: 11266364]
45. Traore K, et al. Redox-regulation of Erk1/2-directed phosphatase by reactive oxygen species: Role in signaling TPA-induced growth arrest in ML-1 cells. Journal of Cellular Physiology. 2008; 216:276–285. [PubMed: 18270969]
46. Wynn TA. Cellular and molecular mechanisms of fibrosis. The Journal of Pathology. 2008; 214:199–210. [PubMed: 18161745]
47. O'Brien TP, Yang GP, Sanders L, Lau LF. Expression of *cyr61*, a growth factor-inducible immediate-early gene. Mol. Cell. Biol. 1990; 10:3569–3577. [PubMed: 2355916]
48. Iyer VR, et al. The transcriptional program in the response of human fibroblasts to serum. Science. 1999; 283:83–87. [PubMed: 9872747]

49. Hanna M, et al. Mechanical regulation of the proangiogenic factor CCN1/CYR61 gene requires the combined activities of MRTF-A and CREB-binding protein histone acetyltransferase. J. Biol. Chem. 2009; 284:23125–23136. [PubMed: 19542562]
50. Sisco M, et al. Antisense inhibition of connective tissue growth factor (CTGF/CCN2) mRNA limits hypertrophic scarring without affecting wound healing in vivo. Wound. Repair Regen. 2008; 16:661–673. [PubMed: 19128261]
51. Brigstock DR. Connective tissue growth factor (CCN2, CTGF) and organ fibrosis: lessons from transgenic animals. J. Cell Commun. Signal. 2009 Epub ahead of print.
52. Ushio-Fukai M. Compartmentalization of redox signaling through NADPH oxidase-derived ROS. Antioxid. Redox. Signal. 2009; 11:1289–1299. [PubMed: 18999986]
53. Castro P, Giri D, Lamb D, Ittmann M. Cellular senescence in the pathogenesis of benign prostatic hyperplasia. Prostate. 2003; 55:30–38. [PubMed: 12640658]
54. Sakamoto S, et al. Increased expression of CYR61, an extracellular matrix signaling protein, in human benign prostatic hyperplasia and its regulation by lysophosphatidic acid. Endocrinology. 2004; 145:2929–2940. [PubMed: 14988385]
55. Quan T, et al. Elevated cysteine-rich 61 mediates aberrant collagen homeostasis in chronologically aged and photoaged human skin. Am. J. Pathol. 2006; 169:482–490. [PubMed: 16877350]
56. Littlewood TD, Bennett MR. Foxing smooth muscle cells: FOXO3a-CYR61 connection. Circ. Res. 2007; 100:302–304. [PubMed: 17307969]
57. Franzen CA, et al. The Matrix Protein CCN1 is Critical for Prostate Carcinoma Cell Proliferation and TRAIL-Induced Apoptosis. Mol. Cancer Res. 2009; 7:1045–1055. [PubMed: 19584265]
58. Chien W, et al. Cyr61 suppresses growth of human endometrial cancer cells. J Biol. Chem. 2004; 279:53087–53096. [PubMed: 15471875]
59. Wang B, Ren J, Ooi LL, Chong SS, Lee CG. Dinucleotide repeats negatively modulate the promoter activity of Cyr61 and is unstable in hepatocellular carcinoma patients. Oncogene. 2005; 24:3999–4008. [PubMed: 15782120]
60. Mori A, et al. CYR61: a new measure of lung cancer outcome. Cancer Invest. 2007; 25:738–741. [PubMed: 18058471]
61. Dobroff AS, et al. Silencing cAMP-response element binding protein (CREB) identifies cysteine-rich protein 61 (CYR61) as a tumor suppressor gene in melanoma. J. Biol. Chem. 2009
62. Debacq-Chainiaux F, Erusalimsky JD, Campisi J, Toussaint O. Protocols to detect senescence-associated beta-galactosidase (SA-β-gal) activity, a biomarker of senescent cells in culture and in vivo. Nat. Protoc. 2009; 4:1798–1806. [PubMed: 20010931]
63. Brummelkamp TR, Bernards R, Agami R. A system for stable expression of short interfering RNAs in mammalian cells. Science. 2002; 296:550–553. [PubMed: 11910072]
64. Schomber T, Kalberer CP, Wodnar-Filipowicz A, Skoda RC. Gene silencing by lentivirus-mediated delivery of siRNA in human CD34+ cells. Blood. 2004; 103:4511–4513. [PubMed: 14988151]
65. Sablina AA, et al. The antioxidant function of the p53 tumor suppressor. Nat. Med. 2005; 11:1306–1313. [PubMed: 16286925]
66. Narita M, et al. A novel role for high-mobility group a proteins in cellular senescence and heterochromatin formation. Cell. 2006; 126:503–514. [PubMed: 16901784]
67. Luo JD, Wang YY, Fu WL, Wu J, Chen AF. Gene therapy of endothelial nitric oxide synthase and manganese superoxide dismutase restores delayed wound healing in type 1 diabetic mice. Circulation. 2004; 110:2484–2493. [PubMed: 15262829]
68. Wilson L, Fathke C, Isik F. Tissue dispersion and flow cytometry for the cellular analysis of wound healing. Biotechniques. 2002; 32:548–551. [PubMed: 11911658]
69. Edwards CA, O'Brien J. Modified assay for determination of hydroxyproline in tissue hydrolyzate. Clinica Chimica Acta. 1980; 104:161–167.

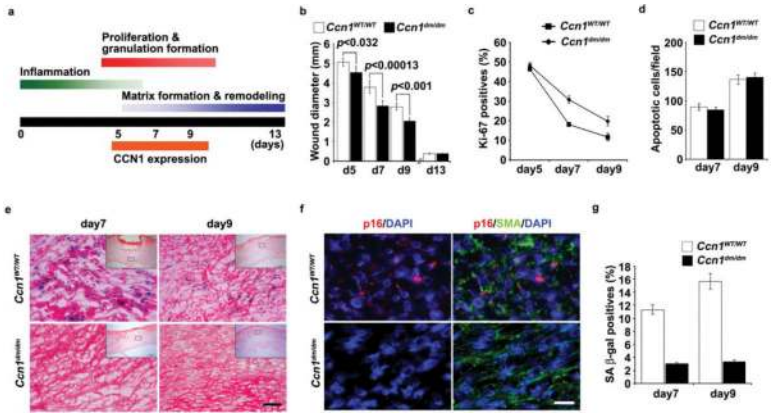

Figure 1. Impaired accumulation of senescent cells in *Ccn1*$^{dm/dm}$ mice during cutaneous wound healing

Excisional cutaneous wounds were created using a 6 mm biopsy punch in *Ccn1*$^{WT/WT}$ (n=5) and *Ccn1*$^{dm/dm}$ mice (n=5). **(a)** Time course of *Ccn1* expression and overlapping phases of healing events. **(b)** Wound closure rate was monitored by measuring wound diameters on indicated days post-wounding. **(c)** The numbers of Ki-67-positive cells were counted as a percentage of Hematoxylin-positive nuclei in 5 randomly selected high-powered fields in frozen sections of granulation tissues, and **(d)** the numbers of apoptotic cells were counted after TUNEL staining. **(e)** Granulation tissues 7 and 9 days post-wounding were stained for SA-β-gal activity, and counterstained with Eosin. Inserts show the entire wound sections and the boxes indicate the enlarged areas. SA-β-gal positive cells were prominent in WT wounds but virtually undetectable in *Ccn1*$^{dm/dm}$ wounds. Similar results were observed in another independently-derived *Ccn1*$^{dm/dm}$ knockin mouse line. Scale bar = 50 μm. **(f)** Granulation tissues 9 days post-wounding were double-stained for p16^{INK4a} (red) and α-SMA (green) by immunofluorescence, and counterstained with DAPI (blue). **(g)** Cells isolated from 7- and 9-day wounds were plated in 60 mm dishes and stained for SA-β-gal activity 2 days later (n=3).

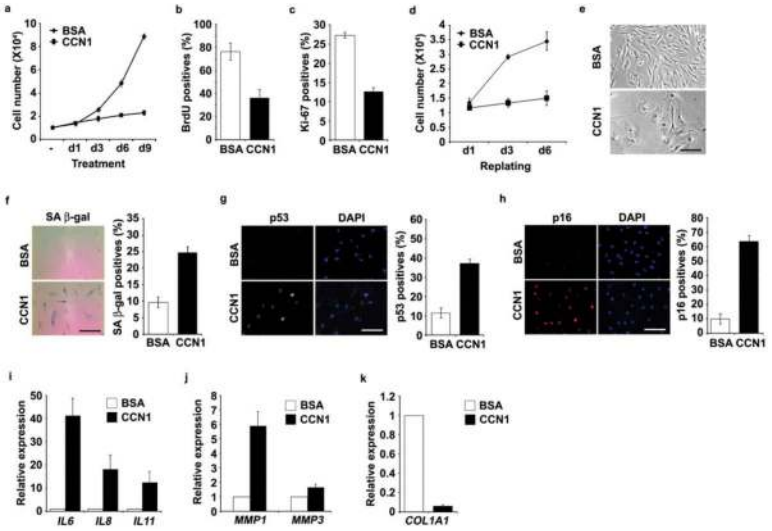

Figure 2. CCN1 induces senescence in normal human fibroblasts

Young human BJ fibroblasts were treated with purified recombinant CCN1 protein (2.5 μg/ml). **(a)** Cells grown in the presence of BSA or CCN1 for indicated days were counted using a hemocytometer. After indicated treatments for 3 days, cells were subjected to either BrdU incorporation assay **(b)** or immunostaining for Ki-67 **(c)**. BrdU or Ki-67 positive cells were counted and expressed as percentages of total number of cells in 10 randomly selected fields. **(d)** Cells were treated with CCN1 or BSA for 6 days, harvested by trypsinization and replated in full growth media. Cell proliferation was monitored by counting cell numbers. **(e)** Morphology of cells treated with CCN1. **(f)** SA-β-gal assay was performed and representative photomicrograph of cells (*left*) and quantification (*right*) are shown. Cells were subjected to immunofluorescence staining for p53 **(g)** or $p16^{INK4a}$ **(h)**, and DAPI was used for counterstaining. Quantifications are shown on the right panels. **(i–k)** Cells were treated with CCN1 for 6 days and qRT-PCR was used to quantify the expression of proinflammatory cytokines (*IL6, IL8, IL11*), matrix degrading enzymes (*MMP1, MMP3*), and collagen 1 (*COL1A1*). Data represent mean ± S.D. of triplicate experiments. Scale bar = 100 μm.

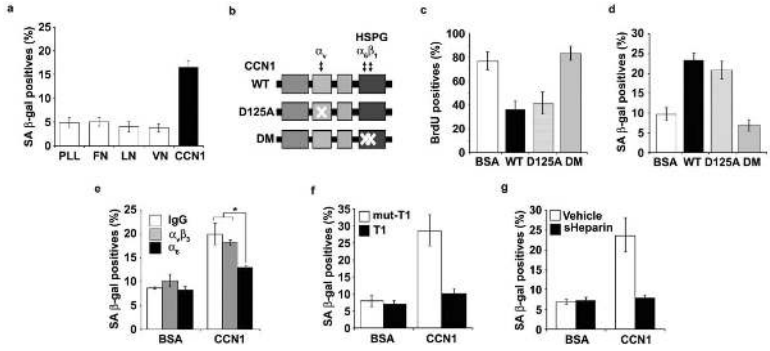

Figure 3. CCN1 induces senescence through integrin $\alpha_6\beta_1$-HSPGs

(a) Cells were adhered to dishes coated with ECM proteins including fibronectin (FN; 10 μg/ml), vitronectin (VN; 5 μg/ml), laminin (LN; 1 μg/ml), CCN1 (5 μg/ml) and poly-L-Lysine (PLL; 10 μg/ml), and stained for SA-β-gal after 3 days. **(b)** Schematic diagram of CCN1 showing the domain structure and the D125A[30] and DM[26] mutants, which are disrupted in binding sites for α_v and $\alpha_6\beta_1$-HSPG, respectively. **(c)** Cells were treated with either WT or mutant CCN1 proteins (2.5 μg/ml each) for 3 days and subjected to BrdU incorporation assay, and **(d)**, SA-β-gal assay. **(e)** Cells were pre-incubated with function-blocking mAbs (50 μg/ml) against $\alpha_v\beta_3$ (LM609) or α_6 (GoH3), and assayed for SA-β-gal. **(f)** Cells were treated with CCN1 with either the $\alpha_6\beta_1$-binding T1 peptide or the non-binding mutant (mut-T1; 0.5 mM each)[27, 33] as a competitor, and SA-β-gal measured. **(g)** soluble heparin (1 mg/ml) was added 1 h before CCN1 treatment, and SA-β-gal assayed. Experiments were done in triplicates and data presented as means ± S.D. (*p<0.004).

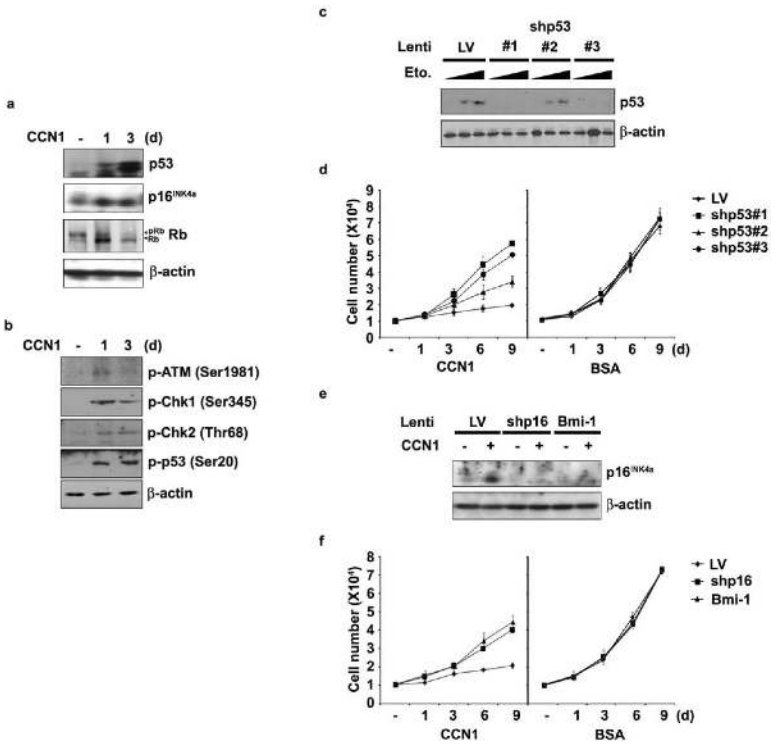

Figure 4. Both p53 and p16^{INK4a} participate in CCN1-induced senescence

(a) BJ cells were treated with CCN1 for indicated times, and expression of p53, p16^{INK4a}, pRb, and β-actin was analyzed by immunoblotting. **(b)** Proteins involved in DDR, including phosphorylated forms of ATM (Ser1981), Chk1 (Ser345), Chk2 (Thr68), and p53 (Ser20) were detected by immunoblotting. **(c)** Cells were infected with three independent lentiviruses driving shRNAs against p53 (#1, 2 and 3). The effectiveness of knockdown was shown in cells treated with etoposide for 6 hrs (Eto; 20 or 50 μM) to induce p53. Cells infected with empty lentivirus (LV) were used as controls. **(d)** Cells infected as above were either treated with CCN1 or BSA and cell numbers were counted at indicated days. **(e)** Cells were infected with lentivirus expressing Bmi-1 or shRNA against p16^{INK4a}, and **(f)** were either treated with CCN1 or BSA and cell numbers counted. Experiments were done in triplicates and data presented as means ± S.D.

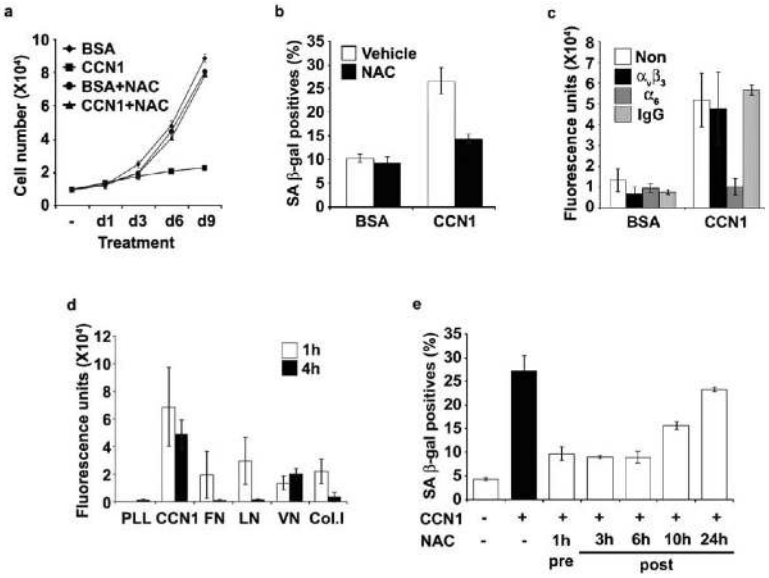

Figure 5. Sustained ROS accumulation induced through CCN1-$\alpha_6\beta_1$ interaction is required for senescence

(a) BJ cells were pretreated with NAC (2.5 mM) for 1 h followed by the addition of CCN1. NAC was replenished daily and cell numbers were counted, and **(b)** SA-β-gal expression was evaluated after 3 days. **(c)** Cells were pre-treated with function-blocking mAbs against $\alpha_v\beta_3$ or α_6 (50 μg/ml each) for 1 h, followed by CCN1 treatment for an additional 1 h and stained with H_2DCFDA (10 μM). ROS was quantified by fluorescence measurements. **(d)** Cells were adhered to surfaces coated with PLL or ECM proteins including FN, VN, LN, Collagen I (Col1; 10 μg/ml), and CCN1 as in Fig. 3a, and ROS levels were measured after 1 or 4 h as above. **(e)** Cells were treated with CCN1 and SA β-gal expression was assayed after 3 days. NAC (2.5 mM) was added either 1 h before or 3, 6, 10, and 24 h after CCN1 treatment. All experiments were done in triplicates and data presented as means ± S.D.

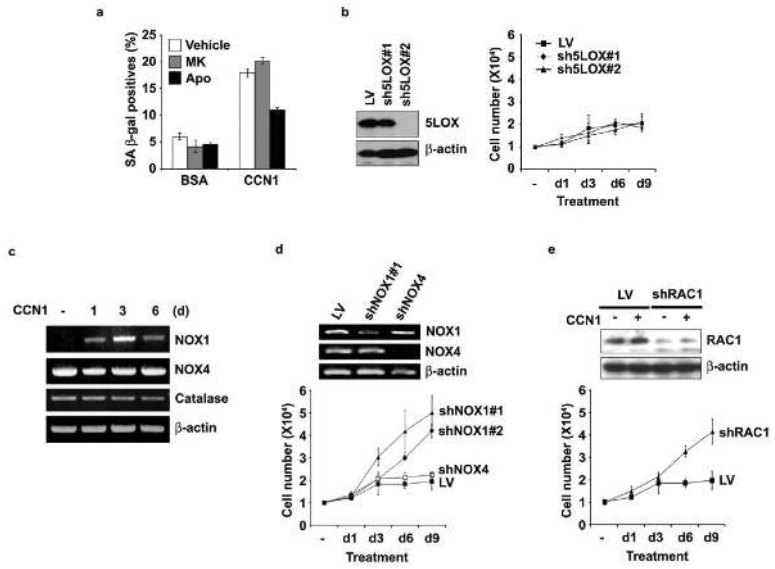

Figure 6. NOX1-RAC1 complex mediates CCN1-induced senescence

(a) BJ cells were preincubated for 1 h with inhibitors of 5-LOX (MK886, 5 μM), NADPH oxidase (apocynin, 10 μM) or vehicle (0.1% DMSO), followed by CCN1 treatment for 3 days and SA-β-gal expression was determined. Chemical inhibitors were replenished daily. **(b)** Cells were infected with lentiviruses encoding shRNAs against 5-LOX (sh5LOX #1 and #2). Knockdown was assessed by immunoblotting (*left*) and cell proliferation after CCN1 treatment was monitored by counting cell numbers (*right*). **(c)** Cells treated with CCN1 for various times were assayed for expression of NOX1, NOX4, catalase and β-actin by RT-PCR. **(d)** Lentiviral shRNA-mediated knockdown of NADPH oxidase 1 (shNOX1 #1 and #2) and 4 (shNOX4) was accomplished as above and confirmed by RT-PCR (*top*). Proliferation of infected cells after CCN1 treatment was determined by counting cell numbers (*bottom*). **(e)** Lentiviral shRNA knockdown of RAC1 (shRAC1) was confirmed by immunoblotting (*top*), and proliferation of knockdown cells after CCN1 treatment was assessed (*bottom*). All experiments were done in triplicates and data presented as means ± S.D.

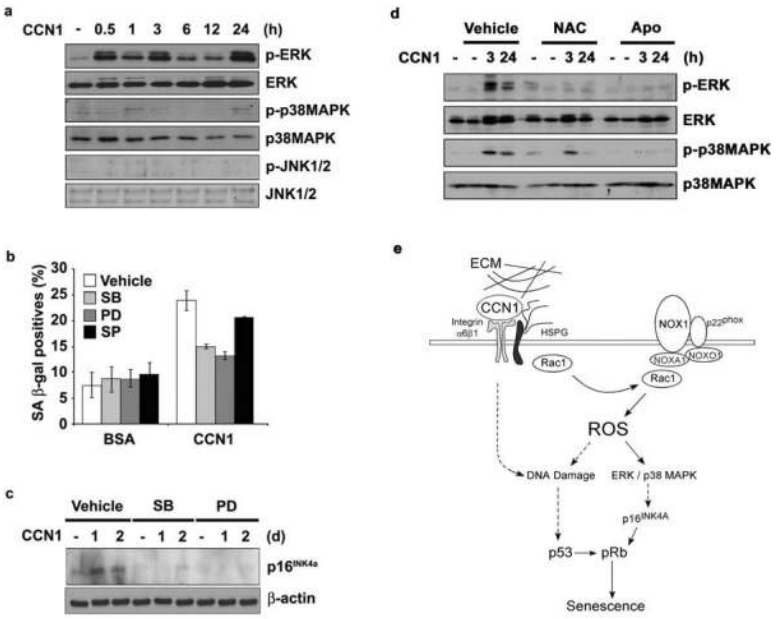

Figure 7. Induction of p16^{INK4a} through ROS-dependent activation of stress kinases

(a) Lysates of BJ cells treated with CCN1 for indicated times were analyzed for the activation of ERK1/2 (p42/p44), p38 MAPK, and JNK1/2 by immunoblotting using their cognate antibodies and phosho-specific antibodies. **(b)** Cells were pre-incubated with inhibitors of either p38MAPK (SBS202190; 10 μM), MEK1 (PD98059; 20 μM), or JNK1/2 (SP600125; 25 μM) for 1 h and then treated with CCN1 (2.5 μg/ml). SA-β-gal expression was assayed three days later. Data presented as means ± S.D. (n=5) **(c)**. Cells pre-incubated with inhibitors as above were then treated with CCN1 for 24 or 48 hrs, and p16^{INK4a} was detected by immunoblotting. **(d)** Activation of both ERK and p38 MAPK by CCN1 was examined in cells pretreated with either NAC (2.5 mM) or apocynin (10 μM) by immunoblotting. **(e)** A signaling model for CCN1-induced senescence. Upon binding to integrin $\alpha_6\beta_1$ and HSPGs, CCN1 activates the RAC1-NOX1 complex to generate a robust and sustained accumulation of ROS, which triggers the biphasic hyperactivation of ERK and p38 MAPK, leading to p16^{INK4a} induction. CCN1 also induces a DDR and activates p53, in part through a ROS-dependent mechanism. Both p53 and p16^{INK4a} contribute to CCN1-induced senescence.

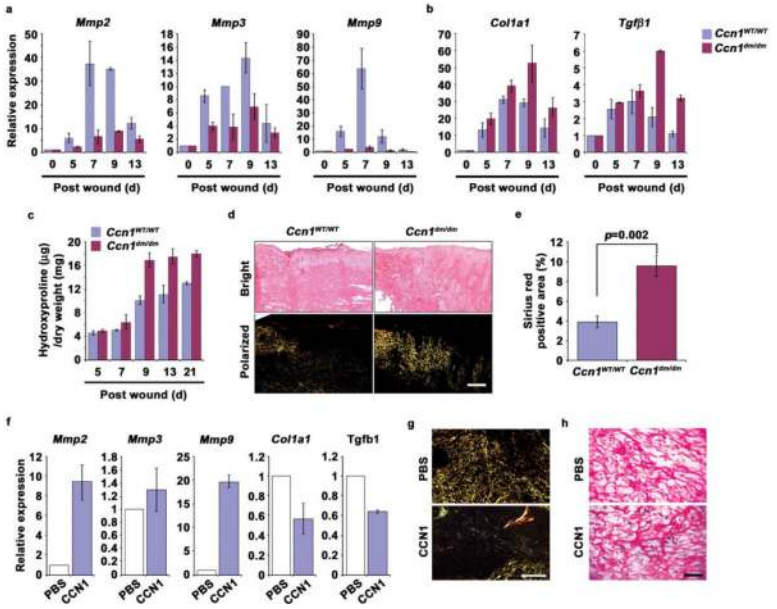

Figure 8. Enhanced fibrogenic response during wound healing *in Ccn1*$^{dm/dm}$ mice

Gene expression in granulation tissues from WT and *Ccn1*$^{dm/dm}$ mice 5–13 days post-wounding was analyzed by qRT-PCR. Relative expression of **(a)** *Mmp2*, *Mmp3*, *Mmp9*, and **(b)** *Col1a1* and *Tgfβ1* is shown. **(c)** Total amount of hydroxyproline in healing wounds isolated 5–21 days post-wounding from WT and *Ccn1*$^{dm/dm}$ mice was determined and normalized over the total dry weight of the tissue. **(d)** Frozen sections from tissues 9 days post-wounding were stained with Sirius red for collagen. Images were acquired from bright field (*top*) and under polarized light (*bottom*). Scale bar = 100 μm. **(e)** Sirius red-positive area was calculated from at least 3 adjacent sections using ImageJ software. All experiments were done in triplicates and data presented as means ± S.D. **(f)** Purified recombinant CCN1 protein (0.1 mg/ml; 50 μl per dose) in PBS or PBS alone was topically applied to excisional wounds of *Ccn1*$^{dm/dm}$ mice daily, and wound granulation tissue harvested 9 days post wounding and analyzed by qRT-PCR (n=5). **(g)** Wounds so treated were sectioned and stained with Sirius red and visualized under polarized light (scale bar = 100 μm), and **(h)** stained for SA-β-gal (scale bar = 50 μm).